Heliyon 9 (2023) e19680

Contents lists available at ScienceDirect

Heliyon

journal homepage: www.cell.com/heliyon

# Identification of m$^5$C-related molecular subtypes and prediction models in the prognosis and tumor microenvironment infiltration of soft tissue sarcoma

Xianfeng Wang [a], Yicheng Mao [b], Hanlu Xu [b], Jiyang Chen [b], Xiao chen [a,*]

[a] Department of Orthopedics, Suzhou Hospital of Anhui Medical University, Suzhou, 234000, Anhui, China
[b] Wenzhou Medical University, Wenzhou, 325000, Wenzhou, China

ARTICLE INFO

*Keywords:*
m$^5$C methylation
Immune cell infiltration
Tumor microenvironment
Prognostic signature
Soft tissue sarcoma

ABSTRACT

*Background:* The epigenetic regulator in cancer progression and immune response has been demonstrated recently. However, the potential implications of 5-methylcytosine (m$^5$C) in soft tissue sarcoma (STS) are unclear.

*Methods:* The RNA sequence profile of 911 normal and 259 primary STS tissues were obtained from GTEx and TCGA databases, respectively. We systematically analyzed the m$^5$C modification patterns of STS samples based on 11 m$^5$C regulators, and comprehensively correlated these modification patterns with clinical characteristics, prognosis, and tumor microenvironment (TME) cell-infiltrating. Furthermore, an m$^5$C-related signature was generated using Cox proportional hazard model and validated by the GSE17118 cohort.

*Results:* Two distinct m$^5$C modification patterns (cluster1/2) were discovered. The cluster1 had favorable overall survival, higher immune score, higher expression of most immune checkpoints, and active immune cell infiltration. The GSVA analysis of the P53 pathway, Wnt signaling pathway, G2M checkpoint, mTORC1 signaling, Wnt/β catenin signaling, and PI3K/AKT/mTOR signaling were significantly enriched in the cluster2. Moreover, 1220 genes were differentially expressed between two clusters, and a m$^5$C prognostic signature was constructed with five m$^5$C-related genes. The signature represented an independent prognostic factor and showed the favorable performance in the GSE17118 cohort. Patients in the low-risk group showed higher immunoscore and higher expression of most immune checkpoints. Further GSVA analysis indicated that the levels of P53 pathway, Wnt signaling pathway, and TGF-β signaling pathway were different between low- and high-risk groups. Moreover, a nomogram incorporating m$^5$C signature and clinical variables was established and showed well performance.

*Conclusion:* This work showed that the m$^5$C modification plays a significant role in the progression of STS and the formation of TME diversity. Evaluating the m$^5$C modification pattern of tumor will enhance our cognition of TME infiltration characterization to guide more effective immunotherapy strategies.

* Corresponding author. Department of Orthopedics, Suzhou Hospital of Anhui Medical University, Suzhou, 234000, Anhui, China.
*E-mail address:* chenx90082866@163.com (X. chen).

https://doi.org/10.1016/j.heliyon.2023.e19680
Received 26 March 2023; Received in revised form 28 August 2023; Accepted 30 August 2023
Available online 1 September 2023

## 1. Introduction

Soft tissue sarcoma (STS) represents a heterogeneous collection of malignant tumors that occur primarily in the mesenchymal tissues, such as muscle and adipose tissues [1]. Although STS only accounts for roughly 1% of all human malignancies (12,750 new cases and 5270 deaths in the United States in 2019) [2,3], it accounts for approximately 10% of malignancies in children and adolescents [4,5]. Surgery, chemotherapy, and palliative radiotherapy are still the preferred treatment methods [6,7], and other novel and effective treatment methods are intensively being explored [8,9]. Even if the treatment regimen is intensified or new drugs are added, the prognosis for STS is still poor, especially for advanced patients whoes 5-year survival rate reduced ignificantly, and was only 27.2% [10]. So far, the pathogenesis and progression of STS remains unclear, which limits the innovation of targeted therapy. Therefore, it is necessary to elucidate the pathogenesis and progression of STS from different perspectives.

Epigenetic regulation is fundamentally involved in transcriptional regulation, and is critical for genomic integrity, cell proliferation, and cell fate [11]. In addition to DNA methylation and histone modification, reversible RNA modification has been confirmed to be another important factor in gene expression regulation [12]. 5-Methylcytosine ($m^5C$) was first identified in stable and abundant tRNAs and rRNAs [13], and its regulatory role in mRNA has been explored recently [14,15]. Yang et al. [14] revealed that $m^5C$ modification is enriched in CG-rich regions as well as regions immediately downstream of translation initiation sites, showing dynamic and tissue-specific features. Notably, increasing evidence demonstrated that mRNA $m^5C$ plays a crucial role in a variety of biological behaviors, including mRNA alternative splicing, export, localization and translation [16,17]. Similar to the modification of $m^6A$ [18], $m^5C$ is manipulated by three types of regulators, including "writer" (methyltransferase), "reader" (binding or recognition protein), and "eraser" (demethylase). The "writers" (*NSUN1-7*, *DNMT1-2*, and *DNMT3A-B*) catalyze the formation of $m^5C$, the "reader" (*ALYREF*) decodes methylation of $m^5C$, and the "eraser" (*TET2*) selectively removes the methyl code [19–22].

Recently, emerging evidence has shown that the mRNA $m^5C$ is associated with the occurrence, progression, and drug responses of malignant tumors [21]. Chen et al. [15] identified many oncogene RNAs with hypermethylated $m^5C$ sites, which had a causal relationship with their upregulation in the bladder cancer. This demonstrated that *NSUN2* drives the pathogenesis of bladder cancer by

**Table 1**
Baseline characteristics of 259 soft tissue sarcoma patients.

| | Total set(n = 259) |
|---|---|
| Age, years | 60.71 ± 14.59 |
| Race | |
| White | 226(87.3) |
| Black | 18(6.9) |
| Asian | 6(2.3) |
| Unknown | 9(3.5) |
| Sex | |
| Male | 118(45.6) |
| Female | 141(54.5) |
| Tumor site | |
| Extremity | 85(32.8) |
| Other | 174(67.2) |
| Histological type | |
| Leiomyosarcoma | 104(40.2) |
| Dedifferentiated liposarcoma | 58(22.4) |
| UPS | 51(19.7) |
| Myxofibrosarcoma | 25(9.7) |
| Other | 21(8.1) |
| Margin status | |
| R0 | 154(59.5) |
| R1/2 | 78(30.1) |
| Unknown | 27(10.4) |
| Metastasis | |
| No | 120(46.3) |
| Yes | 56(21.6) |
| Unknown | 83(32.0) |
| Multifocal indicator | |
| No | 197(76.1) |
| Yes | 40(15.4) |
| Unknown | 22(8.5) |
| Radiotherapy | |
| No | 140(54.1) |
| Yes | 73(28.2) |
| Unknown | 46(17.8) |
| Pharmacotherapy | |
| No | 176(68.0) |
| Yes | 37(14.3) |
| Unknown | 46(17.8) |

UPS: Undifferentiated pleomorphic sarcoma.

targeting specific $m^5C$ methylation site. In prostate cancer, Frye et al. [23] observed high expression of *NSUN2* in cancer tissues, and identified *NSUN2* as a critical protein in PAR2-mediated cancer cell migration via specific methylation. In addition, Zhang et al. [24] evidenced that the distribution pattern of mRNA $m^5C$ was associated with extensive cellular functions. However, the relationship between $m^5C$ regulators and STS remains unclear, and thus it is necessary to do further research.

This study aimed to explore the correlations of $m^5C$ RNA methylation regulators with prognosis, tumor microenvironment (TME), immune cells infiltration, and immune checkpoints in STS. Clustering subtypes and risk models of $m^5C$ RNA methylation regulators were established to improve prognostic risk stratification of STS patients, thereby facilitating treatment decision making. Additionally, we also explored the mechanisms of the interaction between $m^5C$ RNA methylation regulators and STS using a variety of bioinformatics tools.

## 2. Materials and methods

### 2.1. Data collection and processing

The RNA-sequence data of TCGA-SACR cohort were downloaded from the UCSC Xena browser (https://xenabrowser.net/), which contains 259 primary STS patients. The corresponding clinical information of TCGA-SACR was obtained from the cBioPortal (www.cbioportal.org). The expression data of 911 normal muscle and adipose tissues from GTEx project were also downloaded from the UCSC Xena browser to verify the expression pattern of the $m^5C$ regulators between tumor and normal tissues. For the TCGA and GTEx database, the RNA-sequence data (FPKM values) were normalized into $\log_2(FPKM+1)$. Additionally, the data of the GSE17118 dataset were downloaded from the gene expression omnibus (GEO) database to validate our signature. The baseline information of all patients is summarized in Table 1.

### 2.2. Differential, correlation, and survival analyses of $m^5C$ regulators

Thirteen $m^5C$ regulators were identified from previous published papers, including "writers" (*NSUN1-7*, *DNMT1*, *DNMT2*, *DNMT3A*, and *DNMT3B*), "reader" (*ALYREF*), and "eraser" (*TET2*) [25]. After gene expression profiles of STS and normal tissues were normalized by "LiMMA-normalizeBetweenArrays", the differential expressions of $m^5C$ regulators were evaluated by the Wilcoxon signed-rank test with the "limma" package. Pearson correlation analysis was used to study the correlation between regulators, and was performed separately in tumors and normal tissues. Moreover, the information of expression data and overall survival (OS) was integrated, and the univariate Cox analysis was performed to assess the prognostic value of each regulator. In the present study, except for special instructions, the p-value$<$0.05 (two side) was considered as statistical significance.

### 2.3. Unsupervised clustering for $m^5C$ regulators

In order to explore the potential $m^5C$ modification patterns in STS, unsupervised cluster analysis was performed based on the expression of $m^5C$ regulators to classify patients for further analyses [26]. The number of clusters were determined by the Elbow method and the Gap statistic. The distinct OS outcomes between clusters were compared using the log-rank test and the Kaplan-Meier (K-M) curves. In addition, ImmucellAI and ESTIMATE algorithms were used to quantify the immune cell infiltration and TME score, respectively [27,28]. The differences of clinical characteristics, TME scores, immune checkpoints, and 24 types of immune infiltration cells between clusters were compared.

### 2.4. Gene set variation analysis (GSVA)

To investigate the difference on biological process between $m^5C$ modification patterns, we performed GSVA enrichment analysis using the "GSVA" R package. GSVA, a non-parametric unsupervised analysis method, is commonly used for evaluating the variation in the pathway and biological activity between different samples [29]. In this study, we performed GSVA analysis with the "GSVA" package to investigate the difference in biological activity between distinct $m^5C$ modification clusters, and the gene sets of "c2. cp. kegg.v7.1.-symbols" and "h.all.v7.1. symbols" were obtained from the MsigDB database for GSVA.

### 2.5. Identification of differentially expressed genes (DEGs) between $m^5C$ subtypes

According to results of the unsupervised cluster analysis, we classified 259 STS patients into two distinct $m^5C$ clusters, and the "limma" R package was used to screen DEGs between the two $m^5C$ modification clusters. Genes with FDR$<$0.05 and $|\log_2FC|>1$ were defined as DEGs, namely the $m^5C$-related genes. Then, functional annotations, including Gene Ontology (GO) and Kyoto Encyclopedia of Genes and Genomes (KEGG) analyses, were performed in $m^5C$-related genes using the "clusterProfiler" package, and FDR$<$0.5 was set as the cutoff value.

### 2.6. Construction and external validation of the $m^5C$-related signature

To further understand the prognostic value of $m^5C$-related genes in STS, survival analysis was performed. First, the univariate Cox regression analysis was performed to identify OS-related genes, and the genes meeting the screening criteria of $P < 0.05$ were selected.

Then, we utilized LASSO regression analysis to choose the most significant prognostic genes with the "glmnet" package [30]. Finally, those genes identified from the LASSO regression analysis were incorporated into the multivariate Cox analysis, and an $m^5C$-related signature was constructed. The individual riskScore of each STS patient in the training cohort was calculated according to coefficients and expressions of selected genes, and the equation is shown as follows:

$$riskScore = \sum_{i=0}^{n} Exp_i * Coe_i$$

where① $Exp_i$ is the expression of the selected gene, $Coe_i$ is the estimated regression coefficient of the gene from the multivariate Cox proportional hazards regression analysis, and n is the number of genes.

Using the median riskScore as the cutoff, the patients were divided into low-risk and high-risk groups. The K-M survival curve with the log-rank test was generated to show the difference of OS status between the two groups. Besides, the time-dependent receiver operating characteristic (ROC) curves at 2-, 4-, and 6-years were generated to evaluate the discrimination of the signature with the "survivalROC" package, and the corresponding values of area under the curve (AUC) were calculated simultaneously. Then, the expression data of the genes enrolled in the $m^5C$-related signature were extracted from the GSE17118 dataset to calculate the riskScore. Similarly, the K-M survival and ROC curves were selected to perform external validation.

### 2.7. Construction of a novel nomogram based on the $m^5C$-related signature and clinical prognostic variables

We further explored the independent prognostic role of the $m^5C$-related signature with univariate and multivariate Cox regression analyses. Clinical variables were also incorporated into survival analyses, including age, sex, race, histological type, tumor site, metastasis status, margin status, multifocal indicator, radiotherapy status, and pharmacotherapy status (Supplementary Table 1). Variables with a $P < 0.05$ in the univariate Cox analysis were further included in the multivariate Cox analysis, and independent prognostic variables were identified. Using the "rms" package, a prognostic nomogram based on the $m^5C$-related signature and independent clinical prognostic variables was established. C-index and calibration curves were used to assess the performance of the nomogram.

### 2.8. Statistical analysis

All statistical analyses were performed using R (version 3.6.1). Unpaired Student's t-test, the Wilcoxon rank-sum test, ANOVA, and the Kruskal-Wallis test were used for the comparison of continuous variables. The chi-square test and Fisher's exact test were used to compare categorical variables. Pearson analysis was used for the correlation analyses. p-value <0.05 (two-tailed) was considered as statistical significance.

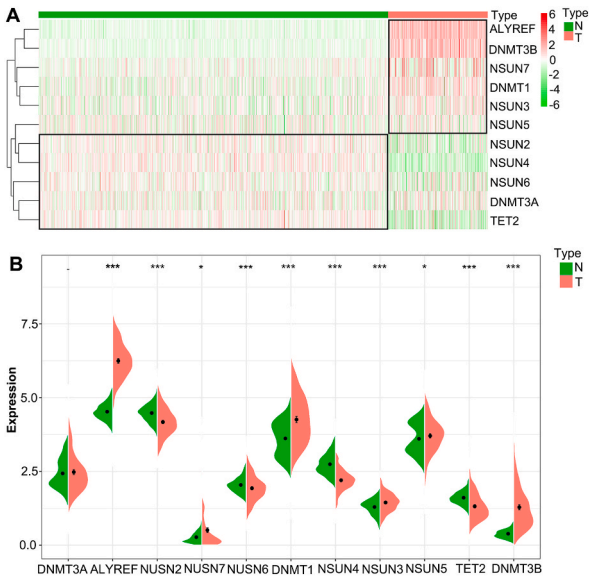


**Fig. 1.** Overeview of 11 $m^5C$ regulators in normal and STS tissues. **(A)** Heatmap showed the expression of 11 $m^5C$ regulators in normal and STS tissues; **(B)** Violin plot showed the difference of $m^5C$ regulators expression between normal and STS tissues.

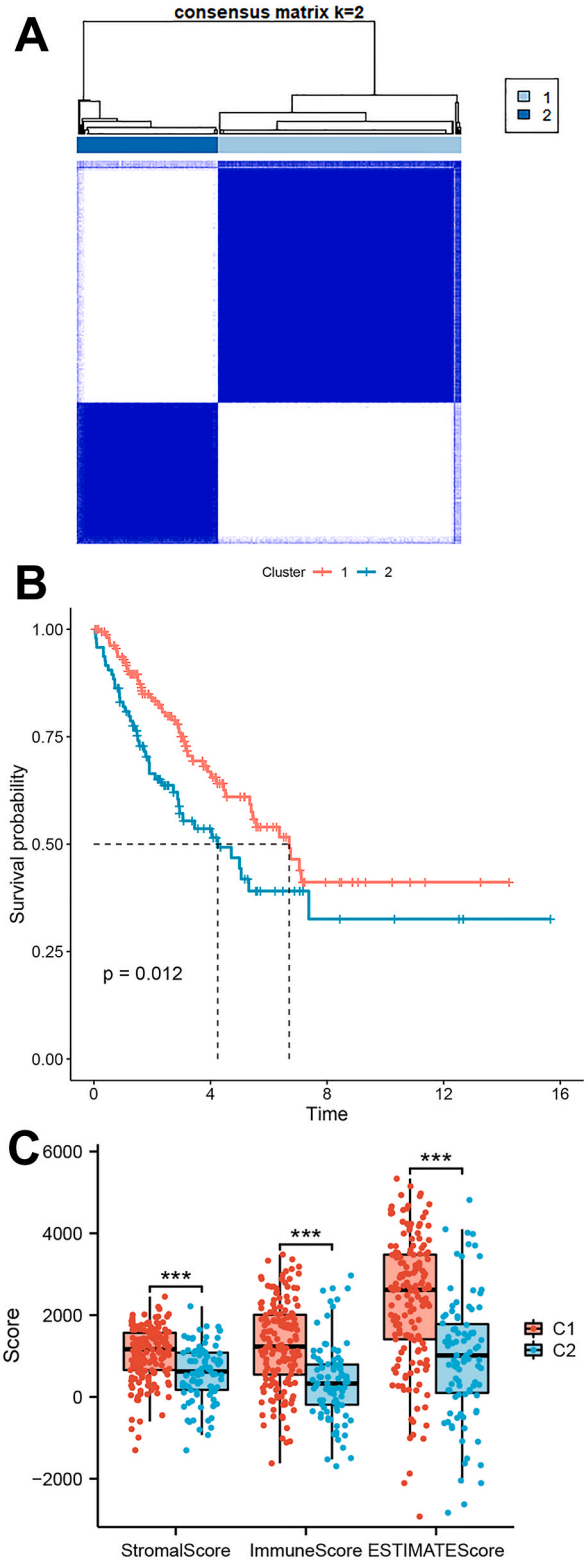


**Fig. 2.** m$^5$C-based clusters significantly associated with prognosis, tumor immune microenvironment and immune checkpoints. **(A)** Consensus matrix heatmap defined two distinct m$^5$C clusters for STS patients; **(B)** Kaplan-Meier survival analysis shows the distinct prognosis of STS between two clusters; **(C)** Stromal score, Immune score, and ESTIMATE score between two m$^5$C modification clusters.

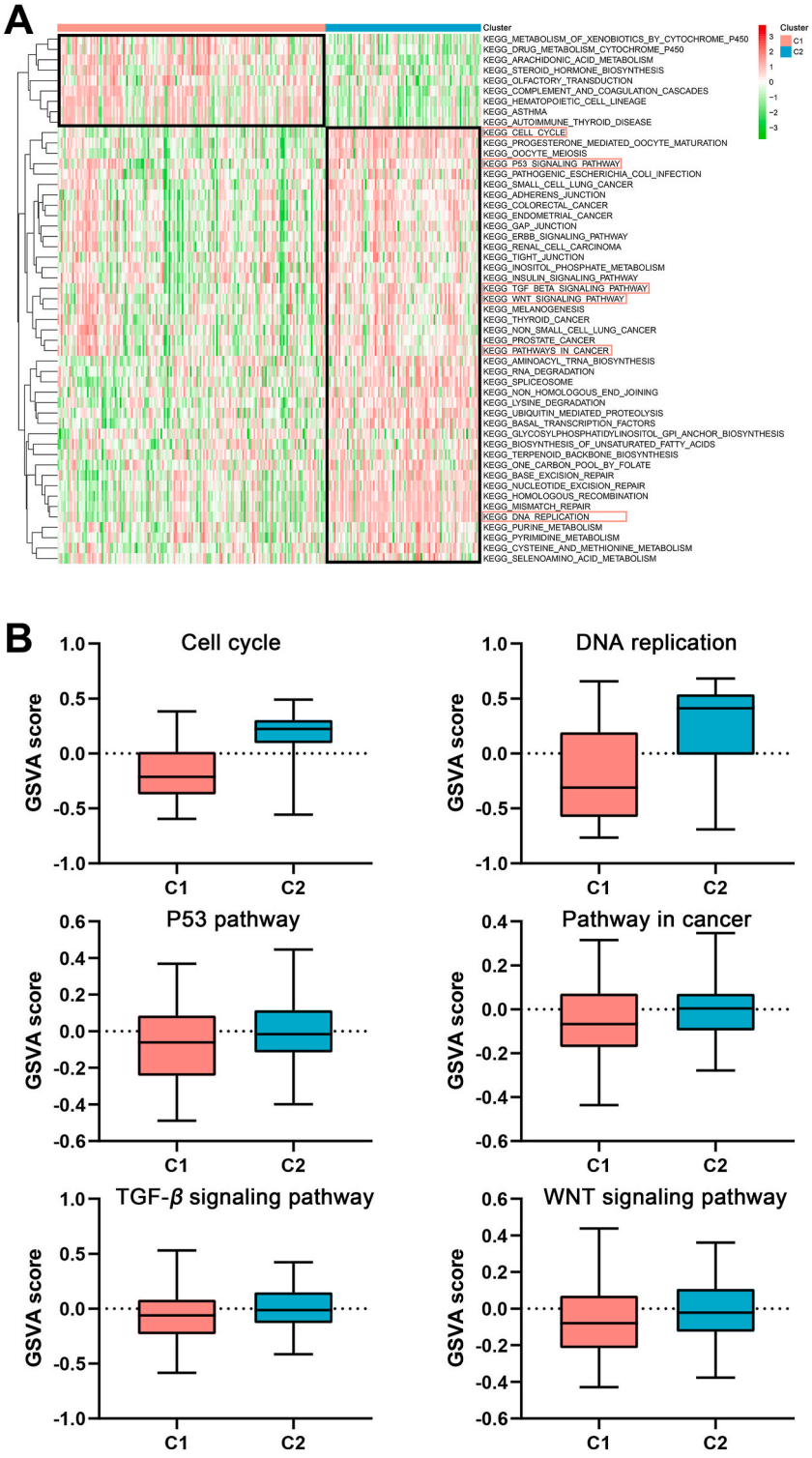


**Fig. 3.** GSVA enrichment analysis showed the activation states of biological pathways in distinct $m^5C$ modification patterns. **(A)** The heatmap showing the GSVA analysis in two clusters; **(B)** The GSVA socre of six pathways closely were associated with tumors.

## 3. Results

### 3.1. Overview of $m^5C$ regulators in normal and STS tissues

Of the 13 $m^5C$ regulators, 11 were found to be expressed in TCGA-SARC and GTEx cohorts, including 9 writers (*NSUN2-7*, *DNMT1*, *DNMT3A*, and *DNMT3B*), 1 reader (*ALYREF*), and 1 eraser (*TET2*). Except for *DNMT3A*, the other 10 $m^5C$ regulators were differentially expressed in STS tissues and normal tissues (Fig. 1A and B). *ALYREF*, *NSUN7*, *DNMT1*, *NSUN3*, *NSUN5*, and *DNMT3B* had higher expression levels in STS tissues, while *NSUN2*, *NSUN6*, *NSUN4*, and *TET2* had lower expression levels in STS tissues (Fig. 1A and B).

The relationships between 11 $m^5C$ regulators were explored by Pearson correlation analysis in STS and normal tissues. As shown in Supplementary Fig. 1A, it was found that not only the same-functional $m^5C$ regulators presented a remarkable correlation, but also among writers, reader, and eraser in normal tissues. However, the significant relationship between each two of them was almost nonexistent in STS tissues. These results indicated that the disruption of the cross-talk between $m^5C$ regulators may play an important role in the oncogenesis of STS. In addition, survival analysis suggested that STS patients with high expression of three genes (*DNMT3A*, *DNMT3B*, and *NSUN6*) had a significantly worse OS, while patients with high expression of *NSUN5* had a favorable OS (Supplementary Fig. 1B).

### 3.2. Two distinct $m^5C$ modification patterns significantly associated with the prognosis and TME characteristics

Two distinct $m^5C$ modification patterns were identified, including 164 cases in cluster1 (C1:63.3%), and 95 cases in cluster2 (C2:36.7%) (Fig. 2A). Survival analysis revealed the particularly prominent OS advantage in the cluster1 ($P = 0.012$) (Fig. 2B). More importantly, the comprehensive bioinformatics analyses suggested that two $m^5C$ modification clusters had distinct TME and immune cell infiltration. The prognosis of the cluster1 with a higher immune, stromal, and ESTIMATE scores was better than that of the cluster2 (Fig. 2C). Additionally, the distribution of sex, histological type, and metastatic status were significantly different between the two clusters (Supplementary Fig. 2). Subsequently, we further analyzed the fraction of 24 immune cell types between two clusters. The results showed that 18 immune cells were significant differences between the two clusters (Supplementary Fig. 3A). The infiltration

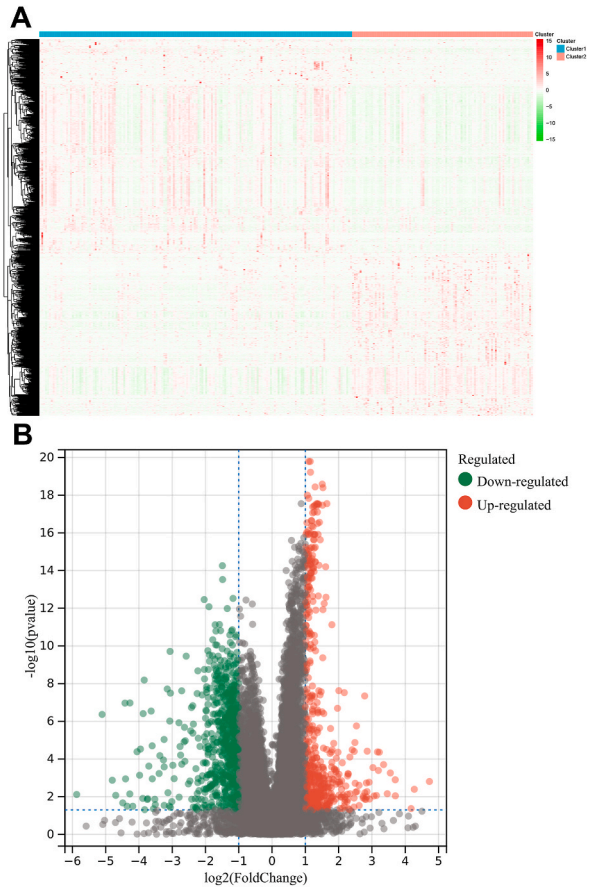


**Fig. 4.** Differential analysis of mRNA between two $m^5C$ clusters. (A) The heatmap showed the 1220 DEGs in normal and STS tissues. **(B)** Volcano plot showed the results of differential expression alaysis between two $m^5C$ clusters.

level of Tc, Tex, Th1, Th2, Tfh, central memory T (Tcm), NkT, MAIT, Macrophage, NK, Tgd(gamma delta T), CD4 T, and CD8 T cells were significantly higher in the cluster 1, while the infiltration levels of CD4 naive, CD8 naive, Tr1, nTreg, iTreg, and Neutrophil cells were significantly lower in cluster 1.

### 3.3. Association of immune checkpoints with $m^5C$ modification patterns

To explore the involvement of immune checkpoints with $m^5C$ modification patterns, we assessed the differential expression of 12 common immune checkpoints in two clusters. A total of 10 immune checkpoints (*PD-1*, *PDL1*, *BTLA*, *CTLA4*, *LAG3*, *PDCD1LG2*, *ICOS*, *CD27*, *HAVCR2*, and *LGALS9*) had higher expression level in the cluster1 (Supplementary Fig. 3B), which indicated that STS patients in cluster1 were more suitable for targeted therapy with immune checkpoint inhibitors. In addition, the prognosis of cluster2 with a higher *PVR* and *VTCN1* was worse than that of the cluster1 ($p < 0.05$) (Supplementary Fig. 3B). Different expression patterns of immune checkpoints suggested that two groups of patients had different susceptibility targeted immunotherapy drugs.

### 3.4. GSVA analysis showing the different biological mechanisms between two $m^5C$ modification clusters

The biological mechanisms between two distinct $m^5C$ modification clusters were further studied by the GSVA analysis. As shown in Fig. 3A–B, cluster1 was markedly enriched in the metabolism of xenobiotics by cytochrome p450, drug metabolism cytochrome p450, arachidonic acid metabolism, steroid hormone biosynthesis, and olfactory transduction. Cluster2 presented enrichment pathways associated with cell cycle, progesterone mediated oocyte maturation, oocyte meiosis, p53 signaling pathway, pathogenic *Escherichia coli* infection based on the top five terms. The results revealed cluster2 was significantly associated with the activation of proliferation, leading to an accelerated progression of STS and poorer OS.

### 3.5. $m^5C$-related DEGs showing distict biological behavior between two modification patterns

To further investigate the potential biological behavior of each $m^5C$ modification pattern, we identified 1220 $m^5C$-related DEGs using the "limma" package (Fig. 4A–B) (Supplementary Table 2). The "clusterProfiler" package was used to perform GO enrichment analysis for the DEGs. For DEGs that upregulated in C1, the most significant GO enriched terms were T cell activation, leukocyte cell-cell adhesion, and leukocyte proliferation; external side of plasma membrane, specific granule, and MIHC class II protein complex (CC); and immune receptor activity, cytokine activity, and chemokine activity (MF) (Supplementary Fig. 4). Generally, immune-related terms were significantly enriched in the C1. Several immune-related pathways, such as B cell receptor signaling pathway, Th1 and Th2 cell differentiation, Primary immunodeficiency, Th17 cell differentiation, and NF−kappa B signaling pathway, were enriched in the C1 (Supplementary Fig. 5). Compared with C1 upregulated DEGs, the relationship between C2 upregulated DEGs and immune features was not as strong. It was remarkably enriched in chromosome segregation, nuclear chromosome segregation, and mitotic sister chromatid segregation (BP); chromosome, centromeric region, spindle, and chromosomal region (CC); microtubule binding, DNA-binding transcription activator activity, and RNA polymerase II-specific (MF) based on GO analysis (Supplementary Fig. 6). Additionally, the KEGG analysis of C2 upregulated DEGs were ecriched in cell cycle, p53 signaling pathway, and oocyte meiosis (Supplementary Fig. 7). Generally, these results fully revealed the biological differences between two $m^5C$ modifications clusters, thereby providing the basis for the further research.

### 3.6. Construction and validation of the $m^5C$-related prognostic signature

The above analyses implied the potential application of $m^5C$ regulators in predicting the prognosis of STS. Then, a total of 311 OS-related DEGs were identified by the univariate Cox regression analysis (Supplementary Table 3), and six prognostic genes were selected by LASSO analysis (Supplementary Table 4). Finally, a signature that incorporating five OS-related DEGs (*GPC2*, *RNF182*, *DUSP9*, *TMEM176B*, and *GLIS1*) were constructed using the multivariate Cox proportional hazards model (Table 2). The formula of riskScore was shown as follows: riskScore = 0.1644*expression of *GPC*+0.0992*expression of *RNF182* + 0.0456*expression of *DUSP9*–0.0024*expression of *TMEM176B* + 0.0465*expression of *GLIS1*. The AUC values of signature for predicting 2-, 4-, and 6-year OS were 0.727, 0.705, and 0.709, respectively (Fig. 5A). It indicated that this $m^5C$-related signature was a valuable tool for OS prediction. Additionally, the K-M survival curve indicated that the patients in the high-risk group had a significantly worse OS than those

**Table 2**
The results of Cox analyses for genes in the final signature.

| Gene | Univariate analysis | | | Multivariate analysis | | |
|---|---|---|---|---|---|---|
| | HR | 95%CI | P | HR | 95%CI | P |
| GPC2 | 1.324 | 1.190–1.473 | 0.000 | 1.179 | 1.026–1.355 | 0.021 |
| RNF182 | 1.121 | 1.070–1.175 | 0.000 | 1.097 | 1.036–1.160 | 0.001 |
| DUSP9 | 1.100 | 1.063–1.139 | 0.000 | 1.047 | 0.998–1.098 | 0.060 |
| TMEM176B | 0.995 | 0.993–0.998 | 0.000 | 0.998 | 0.995–1.000 | 0.079 |
| GLIS1 | 1.072 | 1.033–1.113 | 0.000 | 1.048 | 1.004–1.093 | 0.030 |

HR: hazard ratio; CI: confidence interval.

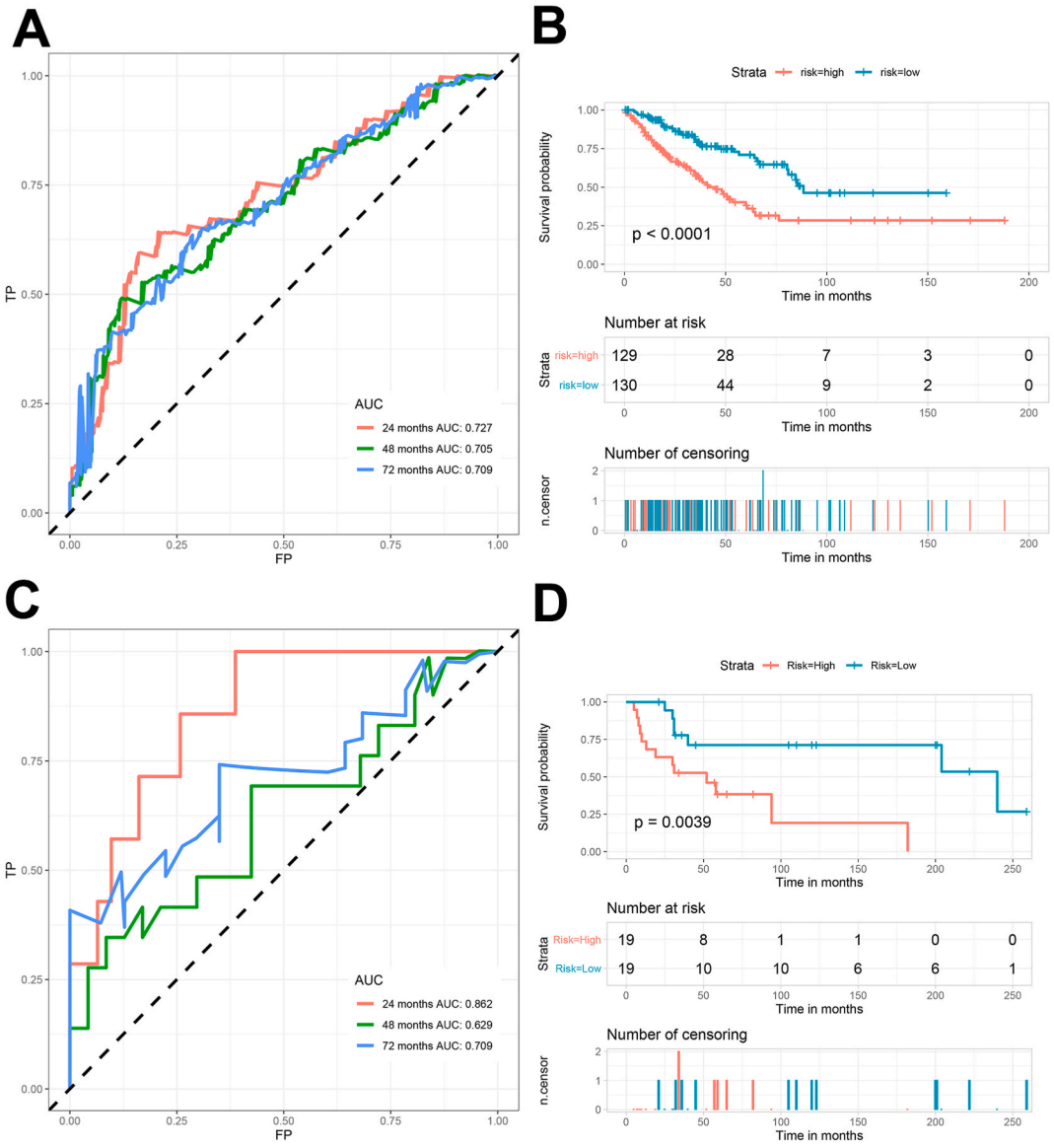


**Fig. 5.** Construction and external validation of the m$^5$C-related signature for STS. **(A)** Time-dependent ROC curves of the m$^5$C-related signature in the training cohort. The AUC values at 2-, 4-, and 6-years were 0.727, 0.705 and 0.709, respectively; **(B)** K-M survival curve showed the distict prognosis between low- and high-risk STS patients in the training cohort; **(C)** Time-dependent ROC curves of the m$^5$C-related signature in the GSE17118 cohort, and the AUC values at 2-, 4-, and 6-years were 0.862, 0.629, and 0.709, respectively; **(D)** K-M survival curve showed the distict prognosis between low- and high-risk STS patients in the GSE17118 cohort.

in the low-risk group (Fig. 5B). In the independent validation cohort, the 2-, 4-, and 6-year AUC values for the m$^5$C signature were 0.862, 0.629, and 0.709, respectively (Fig. 5C). Similar to the training cohort, high-risk patients in the validation cohort had significantly poor prognosis than low-risk patients (Fig. 5D). Two scatter diagrams were generated to show the survival status of STS patients. With the increase of riskScore, it was found that the survival time of patients was gradually decreased and the survival rate was continuously reduced (Supplementary Figs. 8A and 8B). These results suggested that the risk score that was calculated based on the five m$^5$C-related genes could accurately predict the prognosis of STS patients.

### *3.7. Correlations of the m$^5$C signature with TME, immune checkpoints, and immune cell infiltration in STS*

The relationships between risk scores and immune features were further evaluated. The results showed STS patients in the low-risk group had a higher stromal score, higher immune score, and higher ESTIMATE score (Fig. 6A). For the 12 significant immune checkpoints between two m$^5$C modification clusters, the low-risk group had higher expressions of *PD-1*, *PDL1*, *BTLA*, *CTLA4*,

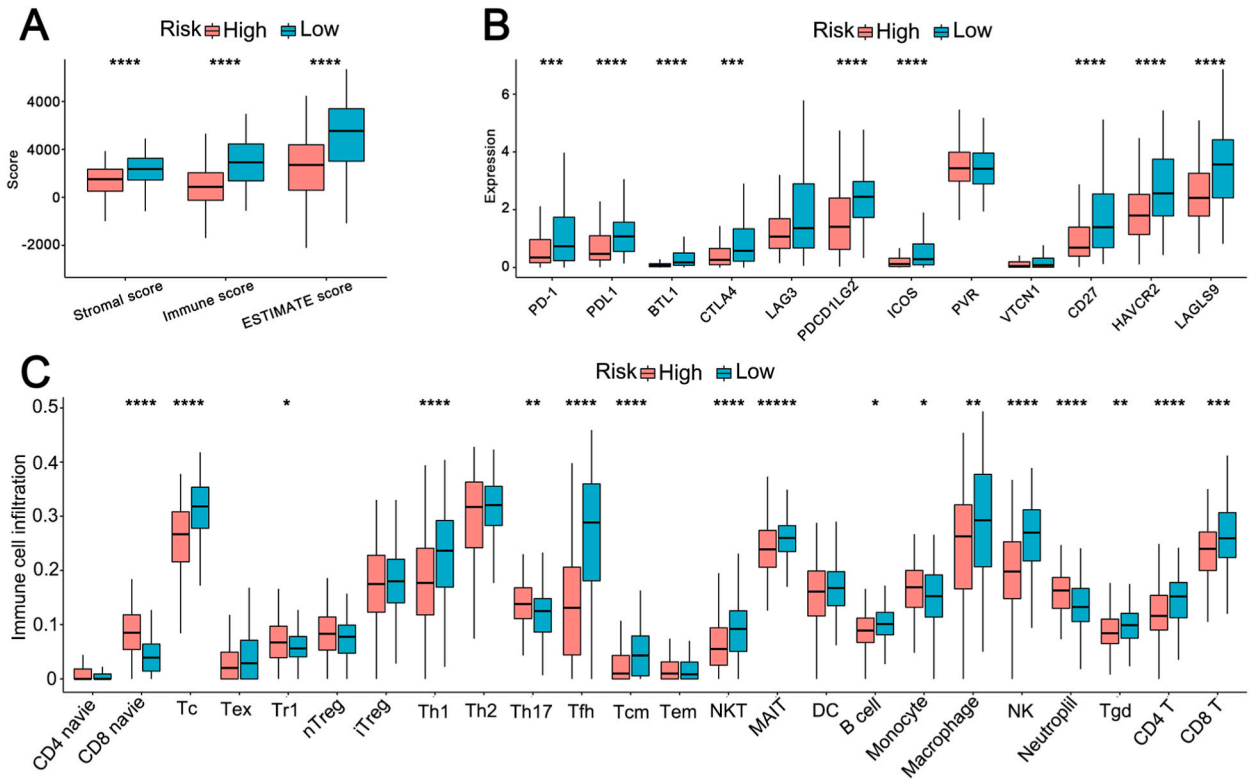


**Fig. 6.** Distinct TME status between low- and high-risk groups. **(A)** Stromal score, Immune score, and ESTIMATE score between low- and high-risk STS patients; **(B)** The differences of immune checkpoints between low- and high-risk STS patients; **(C)** The differences of 24 types of immune cells between low- and high-risk STS patients. STS: soft tissue sarcoma.

*PDCD1LG2*, *ICOS*, and *CD27*, which tended to have the pretty positive response to specific immune checkpoint inhibitors, while the high-risk group tends to be useless (Fig. 6B). We further explored the role of the activated immune system in a better prognosis. STS patients in the low-risk group tended to have a higher infiltration level of Tc, Th1, Tfh, Tcm, NKT, MAIT, B cell, Macrophage, NK, Tgd, CD4 T, and CD8 T, and lower infiltration level of CD8 naive, Tr1, Th17, Monocyte, and Neutrophil (Fig. 6C).

### 3.8. GSVA analysis of low- and high-risk groups

To further investigate the potential biological behavior of low- and high-risk groups, GSVA analysis was performed (Fig. 7). The high-risk group was markedly enriched in the carcinogenic activation pathways, such as P53 signaling pathway, TGF-β signaling pathway, and WNT signaling pathway (Supplementary Figs. 9A–7C). Additionally, several pathways were enriched in the low-risk group, such as the JAK-STAT signaling pathway, regulation of autophagy, and intestinal immune network for IgA production (Supplementary Figs. 9D–9F). Combined with the GSVA analysis in the unsupervised clustering analysis, some important pathways were highly enriched in patients with poor prognosis in both GSVA analyses. Hence, the P53 signaling pathway, TGF-β signaling pathway, and WNT signaling pathway might be implicated in the distinct TME and prognosis of STS patients.

### 3.9. Development of a novel $m^5C$-clinical nomogram

Risk, age, metastatic status, margin status, and multifocal indicator were significantly associated with the OS of STS patients (Fig. 8A). Then, four independent prognostic variables were identified, including risk, age, metastatic status, and margin status (Fig. 8A). A novel $m^5C$-clinical nomogram combining the $m^5C$-related signature and clinical variables was established (Fig. 8B). The nomogram could accurately predict OS, with a C-index of 0.813 by performing bootstrap resampling. In addition, the favorable calibration analysis of the nomogram-predicted OS was highly consistent with the actual outcome at 2-, 4-, and 6-years (Fig. 8C–E).

## 4. Discussion

$m^5C$ is a common modification of both DNA and various cellular RNAs [31,32]. With the recent advance in mapping technologies, the regulatory role of $m^5C$ in mRNAs is beginning to be revealed, and ao far, it has been found that mRNA $m^5C$ plays pivotal regulatory roles across many biological processes, including gene expression, genome editing, cellular differentiation, and organismal

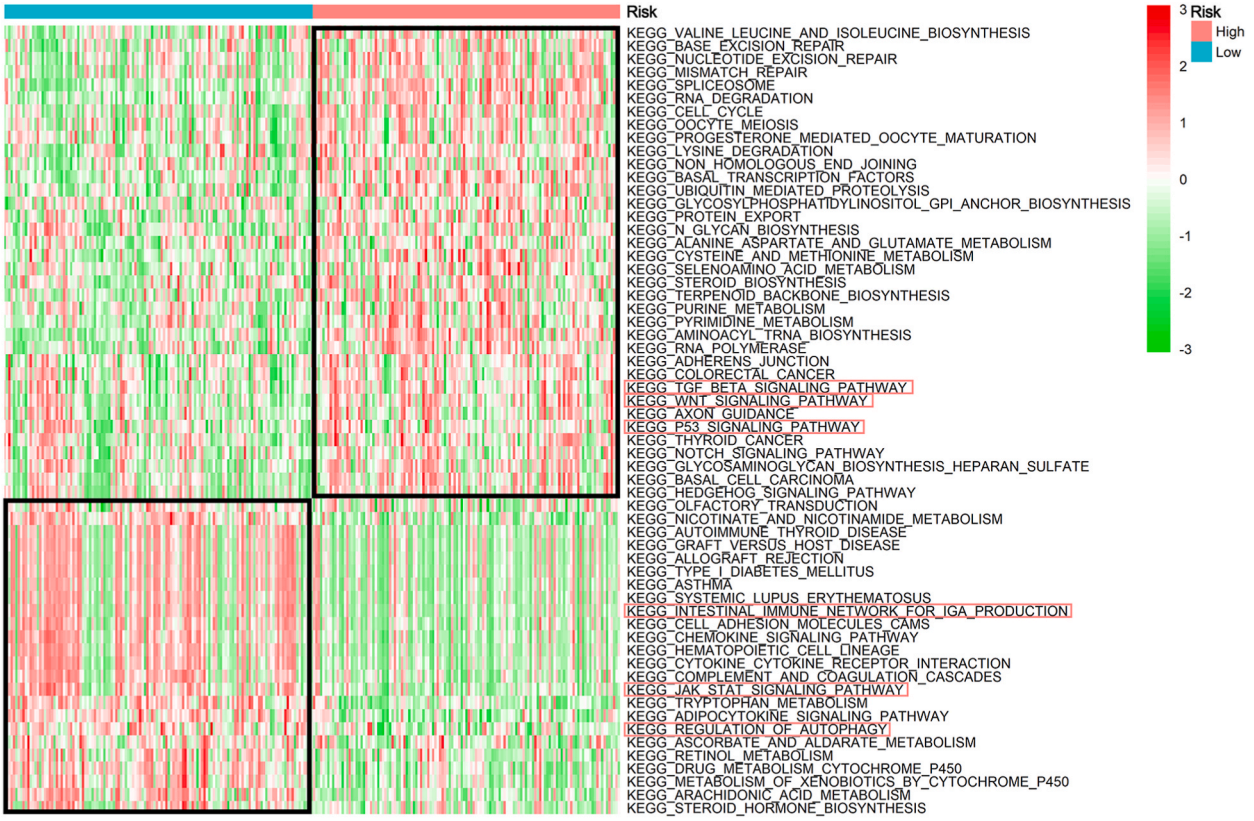


**Fig. 7.** GSVA analysis of low- and high-risk groups. GSVA analysis showing the activation status of biological pathways in two groups; the green spectrum represents inhibited pathways and the red spectrum represents activated pathways.

development [33,34]. However, little is known regarding the relationship between mRNA $m^5C$ and STS, while increasing types of STS have been considered as basically epigenetic diseases with widespread epigenetic dysregulation caused by a small number of genetic changes, or even a single [11,35]. In this study, we applied a series of bioinformatics and machine learning algorithms to demonstrate the key regulatory roles of 11 $m^5C$ regulators in STS, and identified two $m^5C$ modification patterns with distinct TME characteristics and prognosis. Moreover, an $m^5C$-related signature and a comprehensive nomogram were established for prognostic prediction of STS patients.

Previous studies revealed that $m^5C$ regulators play important roles in cell death, developmental defects, and cell proliferation [36,37]. More importantly, anomalous interactions between "writers" and "erasers", arising from alterations to their expression, were found to be linked to malignant tumor pathogenesis and progression [22,38]. Here, 10 of 11 $m^5C$ regulators were differentially expressed between STS and normal tissues. These results indicated a close relationship between these regulators and tumorigenesis. The correlation analyses further suggested that the dysregulation of $m^5C$ regulators in STS. As with STS, several $m^5C$ regulators were abnormally expressed in many malignancies [25,39–41]. For example, the expression of *NSUN2* was downregulated in the lung adenocarcinoma and the expressions of *ALYREF* and *NSUN4* were upregulated in liver cancer [25]. Additionally, the expression of *DNMT1* was upregulated in breast cancer, and *TET2* was downregulated in prostate cancer [42,43]. To explore the reasons, it may be that the damage of normal interactions between $m^5C$ regulators causes the disruption of cellular functions and activation of tumor-related pathways [22,44].

Further, based on the expression of $m^5C$ regulators, we revealed two distinct $m^5C$ modification clusters with remarkably different prognosis and TME characteristics. Cluster1 was characterized by the activation of stroma and immunity with a higher stromal score, immune score, and *ESTIMATE* score, while cluster2 was opposite. Mimicking a similar study reached by Zhang et al. [45] who used unsupervised clustering analysis to identify distinct N6-methyladenosine ($m^6A$) modification patterns, and GSVA enrichment analysis to explore the biological behaviors among these distinct m6A modification patterns in studying potential roles of $m^6A$ modification in TME cell infiltration, we defined cluster1 as "hot-tumor" with significantly better prognosis, and cluster2 as "cold-tumor" with a worse prognosis. It should be pointed out that "hot-tumor" with higher infiltration levels of stromal and immune cells could interfere with signal transduction between tumor cells, disrupt tumor cell metabolism, and finally inhibit tumor growth, invasion, and metastasis [46–48]. The "cold-tumor" with lower infiltration level was associated with immune tolerance and ignorance, and a lack of activated and priming T-cell [49]. Moreover, consistent with the above definitions, we found that 13 of 24 immune cell types have remarkably higher infiltration level in the cluster1. Therefore, our results could draw a conclusion that mRNA $m^5C$ might play a nonnegligible part

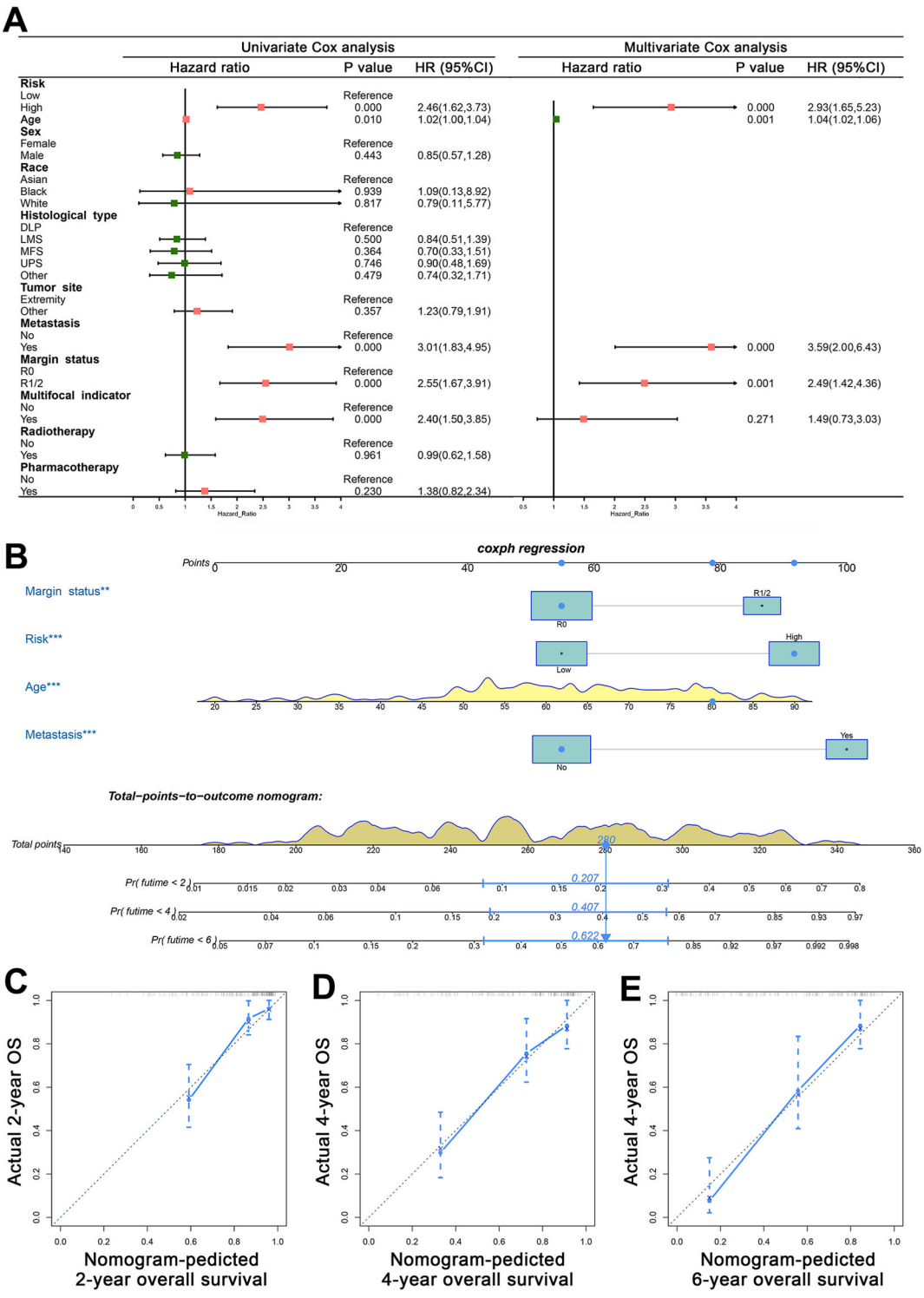


**Fig. 8.** Construction of a novel nomogram based on the m$^5$C-related signature and independent clinical variables. (**A**) Forest plots showed the results of univariate and multivariate Cox analyses of m$^5$C-related signature and independent clinical variables; (**B**) A novel nomogram incorporating m$^5$C-related signature and three clinical variables for the prediction of the overall survival for STS patients. (**C-E**) Calibration curves of the nomogram at 2-, 4-, and 6-years. STS: soft tissue sarcoma.

in shaping individual TME characteristics for STS. Furthermore, in this study, GSVA analysis and function annotation were used to investigate the differences of pathways and biological activities between two clusters. The results were consistent with the TME characteristics of the corresponding cluster. For example, the results of GO analysis revealed cluster1 upregulated genes were primarily enriched in T cell activation, regulation of leukocyte activation, and regulation of lymphocyte activation, which demonstrated the characteristics of "hot-tumor". Thus, mRNA $m^5C$ modification could precisely reflect the infiltration of immune cells and related biological processes, while investigating immune cell distribution in individuals could provide key insights into immune status, tumor progression, and prognosis, as well as therapy [50]. Generally, the above results confirmed the reliability of our distinct $m^5C$ modification clusters for shaping individual TME characteristics of STS.

Recently, tumor-infiltrating immune cells are considered to be the main immune signatures against tumor resistance and are strongly associated with the clinical outcomes of immunotherapies [8,51]. In addition, we gained insight into the role of immune checkpoints in predicting responses to immunotherapy and specific immune checkpoint inhibitors. Several clinical trials are currently testing immune checkpoint inhibitors in STS, but the process is slow and ineffective due to the diversity of STS [52–54]. Joseph et al. [52] explored the efficacy of CTLA-4 with ipilimumab in synovial sarcoma, and most of the patients exhibited radiological evidence of disease progression with little therapeutic effect. Ben-Ami et al. [53] performed a similar clinical trial, no STS patients showed a positive response to the anti-PD-1 antibody nivolumab. However, patients who received anti-PD-L1 (Durvalumab) and anti-CTLA-4 (Tremelimumab) therapy for four cycles had a slight improvement and showed a partial response to combined therapy, which indicated anti-tumor effects require the highly coordinated interaction of multiple immune checkpoint inhibitors. Here, we compressively analyze the expression of 12 immune checkpoints between two distinct $m^5C$ modification clusters. Ten immune checkpoints (*PD-1*, *PDL-1*, *BTLA*, *CTLA4*, *LAG3*, *PDCD1LG2*, *ICOS*, *CD27*, *HAVCR2*, and *LGALS9*) had significantly higher expression level in the cluster1, which indicated that patients in cluster1 might be positively responsive to combination immunotherapy with multiple immune checkpoint inhibitors and tumor-suppressive status [55], and they might have a better prognosis than before. On the contrary, cluster2, defined as "cold-tumor", only had remarkably higher expression of *PVR* and *VTCN1*. Patients in cluster2 might have relatively poor results with immune checkpoint inhibitors, but they could still try targeted therapy for these two immune checkpoints. Combined with the expression of immune checkpoints in each cluster, it confirmed that mRNA $m^5C$ modification patterns could primely affect the therapeutic efficacy of immune checkpoint inhibitors, offering a promise for immunotherapy in individual STS patients.

More importantly, as the $m^5C$ modification was of great importance in shaping distinct TME characteristics from the perspective of mRNA transcriptome, we defined these DEGs between two clusters as $m^5C$-related genes. An $m^5C$-related signature is based on five $m^5C$-related genes (*GPC2*, *RNF182*, *DUSP9*, *TMEM176B*, and *GLIS1*). Of these, *GLIS1* is the most widely studied gene, which is a novel hypoxia-inducible transcription factor and has critical roles in the regulation of multiple physiological processes and diseases [56]. For malignant tumors, *GLIS1* can activate the *WNT5A* to promote breast cancer cell motility [57]. In addition, *GLIS1* has been implicated in the regulation of several other features associated with malignancy, including the risk of relapse and epithelial-mesenchymal transition (EMT) [58]. Therefore, targeting upstream signaling pathways that regulate GLIS1 signaling might offer new therapeutic strategies in the management of cancer [58]. *DUSP9* is a member of the protein tyrosine phosphatases family important for controlling cell growth and cell survival in tumorigenesis [59]. *DUSP9* showed an anticancer effect in clear cell renal cell carcinoma [60], squamous cell carcinoma [61], and hepatocellular carcinoma [62]. The gene appears to play a different role in different tumors. Therefore, we believe that further study on the mechanism of *DUSP9* action in STS will provide better ideas for the further development of targeted therapeutic drugs. The other three genes, *GPC2*, *RNF182*, and *TMEM176B*, are rarely studied. However, our bioinformatics analysis pointed out a promising direction. By performing a further study of effects on STS and even other tumors, we believe that it can promote the research of oncology.

Nevertheless, the present study has some limitations. First, the RNA-seq transcriptome data and corresponding clinical information in this study were obtained from the retrospective cohort (TCGA, GTEx, and GEO databases). Second, we identified the vital regulation roles of mRNA $m^5C$ modification and established an $m^5C$-related signature, which needs further validation in other cohorts with a larger number of patients and patients from different races. Finally, this study provided novel strategies for improving the STS patients' response to immunotherapy by changing the $m^5C$ modification patterns, but further biological experiments and clinical trials are needed to confirm our results.

## 5. Conclusion

In this study, we identified the comprehensive regulation mechanisms of RNA $m^5C$ modification on the TME and prognosis of STS, and established an $m^5C$-related signature based on the five key DEGs. RNA $m^5C$ plays a vital role in shaping individual TME; and targeting the five $m^5C$-related genes or specific $m^5C$ regulators for changing the $m^5C$ modification patterns is the potential strategies to improve personalized immunotherapy in the future.

## Funding

This study is supported by the National College Students Innovation and Entrepreneurship Training Program (No. 202110343028).

## Ethics approval, consent to participate, and consent to publish

Not applicable, because GEO and TCGA belongs to public databases, the patients involved in the database have obtained ethical approval, users can download relevant data for free for research and publish relevant articles, and our study is based on open-source

data, and the Suzhou Hospital of Anhui Medical University do not require research using publicly available data to be submitted for review to their ethics committee, so there are no ethical issues and other conflicts of interest.

## Author contribution statement

Xianfeng Wang: conceived and designed the experiments; performed the experiments; analyzed and interpreted the data; contributed reagents, materials, analysis tools or data; wrote the paper. Xiao Chen: conceived and designed the experiments; wrote the paper. Yicheng Mao, Hanlu Xu, and Jiyang Chen performed the experiments; analyzed and interpreted the data; contributed reagents, materials, analysis tools or data.

## Data availability statement

Data associated with this study has been deposited at Publicly available database analyzed in this study can be found in the Cancer Gernome Altas (https://portal.Gdc.cancer.gov/) and GEO database (https://www.ncbi.nlm.nih.gov/geo).

## Declaration of competing interest

The authors declare that they have no known competing financial interests or personal relationships that could have appeared to influence the work reported in this paper.

## Acknowledgements

We thank everyone who did help in this study. This study is supported by the National College Students Innovation and Entrepreneurship Training Program (No. 202110343028).

## Abbreviations

| | |
|---|---|
| M5C | 5-methylcytosine; |
| STS | soft tissue sarcoma |
| TME | tumor microenvironment |
| GEO | gene expression omnibus |
| OS | overall survival |
| K-M | Kaplan-Meier |
| GSVA | gene set variation analysis |
| DEG | differentially expressed genes |
| GO | Gene Ontology |
| KEGG | Kyoto Encyclopedia of Genes and Genomes |
| ROC | receiver operating characteristic |
| AUC | area under the curve |

## Appendix A. Supplementary data

Supplementary data to this article can be found online at https://doi.org/10.1016/j.heliyon.2023.e19680.

## References

[1] V.Y. Jo, C.D.M. Fletcher, WHO classification of soft tissue tumours: an update based on the 2013 (4th) edition, Pathology 46 (2) (2014), https://doi.org/10.1097/PAT.0000000000000050.
[2] R.L. Siegel, K.D. Miller, A. Jemal, Cancer statistics, 2019, CA A Cancer J. Clin. 69 (1) (2019), https://doi.org/10.3322/caac.21551.
[3] C.A. Stiller, A. Trama, D. Serraino, S. Rossi, C. Navarro, M.D. Chirlaque, P.G. Casali, Descriptive epidemiology of sarcomas in Europe: report from the RARECARE project, Eur. J. Cancer 49 (3) (2013) 684–695, https://doi.org/10.1016/j.ejca.2012.09.011.
[4] C. Wibmer, A. Leithner, N. Zielonke, M. Sperl, R. Windhager, Increasing incidence rates of soft tissue sarcomas? A population-based epidemiologic study and literature review, Ann. Oncol. : official journal of the European Society for Medical Oncology 21 (5) (2010) 1106–1111, https://doi.org/10.1093/annonc/mdp415.
[5] G.Y. Hung, J.L. Horng, Y.S. Lee, H.J. Yen, C.C. Chen, C.Y. Lee, Cancer incidence patterns among children and adolescents in Taiwan from 1995 to 2009: a population-based study, Cancer 120 (22) (2014) 3545–3553.
[6] J.D. Beane, J.C. Yang, D. White, S.M. Steinberg, S.A. Rosenberg, U. Rudloff, Efficacy of adjuvant radiation therapy in the treatment of soft tissue sarcoma of the extremity: 20-year follow-up of a randomized prospective trial, Ann. Surg Oncol. 21 (8) (2014) 2484–2489, https://doi.org/10.1245/s10434-014-3732-4.
[7] I. Judson, J. Verweij, H. Gelderblom, J.T. Hartmann, P. Schöffski, J.-Y. Blay, J.M. Kerst, J. Sufliarsky, J. Whelan, P. Hohenberger, A. Krarup-Hansen, T. Alcindor, S. Marreaud, S. Litière, C. Hermans, C. Fisher, P.C.W. Hogendoorn, A.P. dei Tos, W.T.A. van der Graaf, Doxorubicin alone versus intensified doxorubicin plus ifosfamide for first-line treatment of advanced or metastatic soft-tissue sarcoma: a randomised controlled phase 3 trial, Lancet Oncol. 15 (4) (2014) 415–423, https://doi.org/10.1016/S1470-2045(14)70063-4.

[8] J. Martín-Broto, D. Moura, B. Van Tine, Facts and hopes in immunotherapy of soft tissue sarcomas, Clin. Cancer Res. : an official journal of the American Association for Cancer Research (2020), https://doi.org/10.1158/1078-0432.ccr-19-3335.

[9] A.J. Lazar, M.D. McLellan, M.H. Bailey, C.A. Miller, E.L. Appelbaum, M.G. Cordes, C.C. Fronick, L.A. Fulton, R.S. Fulton, E.R. Mardis, Comprehensive and integrated genomic characterization of adult soft tissue sarcomas, Cell 171 (4) (2017) 950–965.

[10] H.S. Kim, C.M. Nam, S.Y. Jang, S.K. Choi, S.Y. Rha, Characteristics and treatment patterns of patients with advanced soft tissue sarcoma in korea, Cancer Research and Treatment 51 (4) (2019).

[11] B. Nacev, K. Jones, A. Intlekofer, J. Yu, C. Allis, W. Tap, M. Ladanyi, T. Nielsen, The epigenomics of sarcoma, Nat. Rev. Cancer (2020), https://doi.org/10.1038/s41568-020-0288-4.

[12] B.S. Zhao, I.A. Roundtree, C. He, Post-transcriptional gene regulation by mRNA modifications, Nat. Rev. Mol. Cell Biol. 18 (1) (2017) 31–42, https://doi.org/10.1038/nrm.2016.132.

[13] M. Helm, Post-transcriptional nucleotide modification and alternative folding of RNA, Nucleic Acids Res. 34 (2) (2006) 721–733.

[14] X. Yang, Y. Yang, B.-F. Sun, Y.-S. Chen, J.-W. Xu, W.-Y. Lai, A. Li, X. Wang, D.P. Bhattarai, W. Xiao, H.-Y. Sun, Q. Zhu, H.-L. Ma, S. Adhikari, M. Sun, Y.-J. Hao, B. Zhang, C.-M. Huang, N. Huang, G.-B. Jiang, Y.-L. Zhao, H.-L. Wang, Y.-P. Sun, Y.-G. Yang, 5-methylcytosine promotes mRNA export - NSUN2 as the methyltransferase and ALYREF as an mC reader, Cell Res. 27 (5) (2017) 606–625, https://doi.org/10.1038/cr.2017.55.

[15] X. Chen, A. Li, B.-F. Sun, Y. Yang, Y.-N. Han, X. Yuan, R.-X. Chen, W.-S. Wei, Y. Liu, C.-C. Gao, Y.-S. Chen, M. Zhang, X.-D. Ma, Z.-W. Liu, J.-H. Luo, C. Lyu, H.-L. Wang, J. Ma, Y.-L. Zhao, F.-J. Zhou, Y. Huang, D. Xie, Y.-G. Yang, 5-methylcytosine promotes pathogenesis of bladder cancer through stabilizing mRNAs, Nat. Cell Biol. 21 (8) (2019) 978–990, https://doi.org/10.1038/s41556-019-0361-y.

[16] R.-J. Liu, T. Long, J. Li, H. Li, E.-D. Wang, Structural basis for substrate binding and catalytic mechanism of a human RNA:m5C methyltransferase NSun6, Nucleic Acids Res. 45 (11) (2017) 6684–6697, https://doi.org/10.1093/nar/gkx473.

[17] R. Jacob, S. Zander, T. Gutschner, The dark side of the epitranscriptome: chemical modifications in long non-coding RNAs, Int. J. Mol. Sci. 18 (11) (2017), https://doi.org/10.3390/ijms18112387.

[18] C. Zhang, J. Fu, Y. Zhou, A review in research progress concerning m6A methylation and immunoregulation, Front. Immunol. 10 (2019) 922, https://doi.org/10.3389/fimmu.2019.00922.

[19] D. Dominissini, G. Rechavi, 5-methylcytosine mediates nuclear export of mRNA, Cell Res. 27 (6) (2017) 717–719, https://doi.org/10.1038/cr.2017.73.

[20] U. Schumann, H.-N. Zhang, T. Sibbritt, A. Pan, A. Horvath, S. Gross, S.J. Clark, L. Yang, T. Preiss, Multiple links between 5-methylcytosine content of mRNA and translation, BMC Biol. 18 (1) (2020) 40, https://doi.org/10.1186/s12915-020-00769-5.

[21] R. García-Vílchez, A. Sevilla, S. Blanco, Post-transcriptional regulation by cytosine-5 methylation of RNA, Biochim Biophys Acta Gene Regul Mech 1862 (3) (2019) 240–252, https://doi.org/10.1016/j.bbagrm.2018.12.003.

[22] K.E. Bohnsack, C. Höbartner, M.T. Bohnsack, Eukaryotic 5-methylcytosine ($m^5C$) RNA methyltransferases: mechanisms, cellular functions, and links to disease, Genes 10 (2) (2019), https://doi.org/10.3390/genes10020102.

[23] A. Chellamuthu, S.G. Gray, The RNA methyltransferase NSUN2 and its potential roles in cancer, Cells 9 (8) (2020), https://doi.org/10.3390/cells9081758.

[24] Q. Zhang, Q. Zheng, X. Yu, Y. He, W. Guo, Overview of distinct 5-methylcytosine profiles of messenger RNA in human hepatocellular carcinoma and paired adjacent non-tumor tissues, J. Transl. Med. 18 (1) (2020) 245, https://doi.org/10.1186/s12967-020-02417-6.

[25] Y. He, X. Yu, J. Li, Q. Zhang, Q. Zheng, W. Guo, Role of m(5)C-related regulatory genes in the diagnosis and prognosis of hepatocellular carcinoma, Am. J. Tourism Res. 12 (3) (2020) 912–922.

[26] M.D. Wilkerson, D.N. Hayes, ConsensusClusterPlus: a class discovery tool with confidence assessments and item tracking, Bioinformatics 26 (12) (2010) 1572–1573, https://doi.org/10.1093/bioinformatics/btq170.

[27] Y.R. Miao, Q. Zhang, Q. Lei, M. Luo, G.Y. Xie, H. Wang, A.Y. Guo, ImmuCellAI: a unique method for comprehensive T-cell subsets abundance prediction and its application in cancer immunotherapy, Adv. Sci. 7 (7) (2020), 1902880, https://doi.org/10.1002/advs.201902880.

[28] K. Y, M. S, E. M, R. V, H. K, W. T-G, V. T, H. S, P.W. L, L. Da, C. Sl, G. G, K. S-H, M. Gb, R.G. s, Inferring tumour purity and stromal and immune cell admixture from expression data, Nat. Commun. 4 (2013) 2612, https://doi.org/10.1038/ncomms3612.

[29] S. Hänzelmann, R. Castelo, J. Guinney, GSVA: gene set variation analysis for microarray and RNA-seq data, BMC Bioinf. 14 (7) (2013), https://doi.org/10.1186/1471-2105-14-7.

[30] S. Engebretsen, J. Bohlin, Statistical predictions with glmnet, Clin. Epigenet. 11 (1) (2019) 123, https://doi.org/10.1186/s13148-019-0730-1.

[31] X. Yang, Y. Yang, B.F. Sun, Y.S. Chen, J.W. Xu, W.Y. Lai, A. Li, X. Wang, D.P. Bhattarai, W. Xiao, H.Y. Sun, Q. Zhu, H.L. Ma, S. Adhikari, M. Sun, Y.J. Hao, B. Zhang, C.M. Huang, N. Huang, G.B. Jiang, Y.L. Zhao, H.L. Wang, Y.P. Sun, Y.G. Yang, 5-methylcytosine promotes mRNA export - NSUN2 as the methyltransferase and ALYREF as an m(5)C reader, Cell Res. 27 (5) (2017) 606–625, https://doi.org/10.1038/cr.2017.55.

[32] X. Cui, Z. Liang, L. Shen, Q. Zhang, S. Bao, Y. Geng, B. Zhang, V. Leo, L.A. Vardy, T. Lu, X. Gu, H. Yu, 5-Methylcytosine RNA methylation in arabidopsis thaliana, Mol. Plant 10 (11) (2017) 1387–1399, https://doi.org/10.1016/j.molp.2017.09.013.

[33] L. Trixl, A. Lusser, The dynamic RNA modification 5-methylcytosine and its emerging role as an epitranscriptomic mark, Wiley Interdiscip Rev RNA 10 (1) (2019), e1510, https://doi.org/10.1002/wrna.1510.

[34] H. Wu, Y. Zhang, Mechanisms and functions of Tet protein-mediated 5-methylcytosine oxidation, Genes Dev. 25 (23) (2011) 2436–2452, https://doi.org/10.1101/gad.179184.111.

[35] I.-M. Schaefer, G.M. Cote, J.L. Hornick, Contemporary sarcoma diagnosis, genetics, and genomics, J. Clin. Oncol. 36 (2) (2018) 101–110, https://doi.org/10.1200/JCO.2017.74.9374.

[36] J. Song, J. Zhai, E. Bian, Y. Song, J. Yu, C. Ma, Transcriptome-Wide annotation of mC RNA modifications using machine learning, Front. Plant Sci. 9 (2018) 519, https://doi.org/10.3389/fpls.2018.00519.

[37] R. Chhabra, miRNA and methylation: a multifaceted liaison, Chembiochem 16 (2) (2015) 195–203, https://doi.org/10.1002/cbic.201402449.

[38] S. Delaunay, M. Frye, RNA modifications regulating cell fate in cancer, Nat. Cell Biol. 21 (5) (2019) 552–559, https://doi.org/10.1038/s41556-019-0319-0.

[39] Y. Gao, Z. Wang, Y. Zhu, Q. Zhu, Y. Yang, Y. Jin, F. Zhang, L. Jiang, Y. Ye, H. Li, Y. Zhang, H. Liang, S. Xiang, H. Miao, Y. Liu, Y. Hao, NOP2/Sun RNA methyltransferase 2 promotes tumor progression via its interacting partner RPL6 in gallbladder carcinoma, Cancer Sci. 110 (11) (2019) 3510–3519, https://doi.org/10.1111/cas.14190.

[40] M. Manning, Y. Jiang, R. Wang, L. Liu, S. Rode, M. Bonahoom, S. Kim, Z.Q. Yang, Pan-cancer analysis of RNA methyltransferases identifies FTSJ3 as a potential regulator of breast cancer progression, RNA Biol. 17 (4) (2020) 474–486, https://doi.org/10.1080/15476286.2019.1708549.

[41] L. Ye, C. Hu, C. Wang, W. Yu, F. Liu, Z. Chen, Nomogram for predicting the overall survival and cancer-specific survival of patients with extremity liposarcoma: a population-based study, BMC Cancer 20 (1) (2020) 889, https://doi.org/10.1186/s12885-020-07396-x.

[42] H. Liu, Y. Song, H. Qiu, Y. Liu, K. Luo, Y. Yi, G. Jiang, M. Lu, Z. Zhang, J. Yin, Downregulation of FOXO3a by DNMT1 promotes breast cancer stem cell properties and tumorigenesis, Cell Death Differ. 27 (3) (2020) 966–983.

[43] M.L. Nickerson, S. Das, K. Im, S. Turan, S. Berndt, H. Li, H. Lou, S. Brodie, J. Billaud, T. Zhang, TET2 binds the androgen receptor and loss is associated with prostate cancer, Oncogene 36 (15) (2017) 2172–2183.

[44] P. Boccaletto, M.A. Machnicka, E. Purta, P. Piatkowski, B. Baginski, T.K. Wirecki, V. de Crécy-Lagard, R. Ross, P.A. Limbach, A. Kotter, M. Helm, J.M. Bujnicki, MODOMICS: a database of RNA modification pathways. 2017 update, Nucleic Acids Res. 46 (D1) (2018) D303–D307, https://doi.org/10.1093/nar/gkx1030.

[45] B. Zhang, Q. Wu, B. Li, D. Wang, L. Wang, Y.L. Zhou, mA regulator-mediated methylation modification patterns and tumor microenvironment infiltration characterization in gastric cancer, Mol. Cancer 19 (1) (2020) 53, https://doi.org/10.1186/s12943-020-01170-0.

[46] K. Yoshihara, M. Shahmoradgoli, E. Martínez, R. Vegesna, H. Kim, W. Torres-Garcia, V. Treviño, H. Shen, P.W. Laird, D.A. Levine, S.L. Carter, G. Getz, K. Stemke-Hale, G.B. Mills, R.G.W. Verhaak, Inferring tumour purity and stromal and immune cell admixture from expression data, Nat. Commun. 4 (2013) 2612, https://doi.org/10.1038/ncomms3612.

[47] X. Liu, X. Niu, Z. Qiu, A five-gene signature based on stromal/immune scores in the tumor microenvironment and its clinical implications for liver cancer, DNA Cell Biol. (2020), https://doi.org/10.1089/dna.2020.5512.

[48] S.J. Turley, V. Cremasco, J.L. Astarita, Immunological hallmarks of stromal cells in the tumour microenvironment, Nat. Rev. Immunol. 15 (11) (2015) 669–682, https://doi.org/10.1038/nri3902.
[49] J.M. Kim, D.S. Chen, Immune escape to PD-L1/PD-1 blockade: seven steps to success (or failure), Ann. Oncol. : official journal of the European Society for Medical Oncology 27 (8) (2016) 1492–1504, https://doi.org/10.1093/annonc/mdw217.
[50] T.F. Gajewski, H. Schreiber, Y.-X. Fu, Innate and adaptive immune cells in the tumor microenvironment, Nat. Immunol. 14 (10) (2013) 1014–1022, https://doi.org/10.1038/ni.2703.
[51] P.H. Pandya, M.E. Murray, K.E. Pollok, J.L. Renbarger, The immune system in cancer pathogenesis: potential therapeutic approaches, J Immunol Res 2016 (2016), 4273943, https://doi.org/10.1155/2016/4273943.
[52] C.G. Joseph, H. Hwang, Y. Jiao, L.D. Wood, I. Kinde, J. Wu, N. Mandahl, J. Luo, R.H. Hruban, L.A. Diaz, T.-C. He, B. Vogelstein, K.W. Kinzler, F. Mertens, N. Papadopoulos, Exomic analysis of myxoid liposarcomas, synovial sarcomas, and osteosarcomas, Genes Chromosomes Cancer 53 (1) (2014) 15–24, https://doi.org/10.1002/gcc.22114.
[53] E. Ben-Ami, C.M. Barysauskas, S. Solomon, K. Tahlil, R. Malley, M. Hohos, K. Polson, M. Loucks, M. Severgnini, T. Patel, A. Cunningham, S.J. Rodig, F.S. Hodi, J. A. Morgan, P. Merriam, A.J. Wagner, G.I. Shapiro, S. George, Immunotherapy with single agent nivolumab for advanced leiomyosarcoma of the uterus: results of a phase 2 study, Cancer 123 (17) (2017) 3285–3290, https://doi.org/10.1002/cncr.30738.
[54] A.J. Wisdom, Y.M. Mowery, R.F. Riedel, D.G. Kirsch, Rationale and emerging strategies for immune checkpoint blockade in soft tissue sarcoma, Cancer 124 (19) (2018) 3819–3829, https://doi.org/10.1002/cncr.31517.
[55] S.M. Pollack, M. Ingham, M.B. Spraker, G.K. Schwartz, Emerging targeted and immune-based therapies in sarcoma, J. Clin. Oncol. 36 (2) (2018) 125–135, https://doi.org/10.1200/JCO.2017.75.1610.
[56] A.M. Jetten, GLIS1–3 transcription factors: critical roles in the regulation of multiple physiological processes and diseases, Cell. Mol. Life Sci. 75 (19) (2018) 3473–3494.
[57] K. Shimamoto, K. Tanimoto, T. Fukazawa, H. Nakamura, A. Kanai, H. Bono, H. Ono, H. Eguchi, N. Hirohashi, GLIS1, a novel hypoxia-inducible transcription factor, promotes breast cancer cell motility via activation of WNT5A, Carcinogenesis (2020).
[58] A.M. Jetten, Emerging roles of GLI-similar krüppel-like zinc finger transcription factors in leukemia and other cancers, Trends in cancer 5 (9) (2019) 547–557.
[59] A. Bhaduri, R. Sowdhamini, A genome-wide survey of human tyrosine phosphatases, Protein Eng. 16 (12) (2003) 881–888, https://doi.org/10.1093/protein/gzg144.
[60] J. Luo, X. Luo, X. Liu, Z. Fang, J. Xu, L. Li, DUSP9 suppresses proliferation and migration of clear cell renal cell carcinoma via the mTOR pathway, OncoTargets Ther. 13 (2020) 1321–1330, https://doi.org/10.2147/OTT.S239407.
[61] Y. Liu, J. Lagowski, A. Sundholm, A. Sundberg, M. Kulesz-Martin, Microtubule disruption and tumor suppression by mitogen-activated protein kinase phosphatase 4, Cancer Res. 67 (22) (2007) 10711–10719, https://doi.org/10.1158/0008-5472.can-07-1968.
[62] J. Liu, W. Ni, M. Xiao, F. Jiang, R. Ni, Decreased expression and prognostic role of mitogen-activated protein kinase phosphatase 4 in hepatocellular carcinoma, J. Gastrointest. Surg. : official journal of the Society for Surgery of the Alimentary Tract 17 (4) (2013) 756–765, https://doi.org/10.1007/s11605-013-2138-0.